

The Walsh-Hadamard Transform: An Alternative Means of Obtaining Phase and Amplitude Maps

Raimondo Tallia, Piero Morello, and Giancarlo Castellano

Ospedale San Giovanni, and University of Turin, Italy

Currently, Fourier analysis is a method for obtaining the phase and amplitude images used to evaluate abnormalities of cardiac contraction. Since this technique is time-consuming, the present work investigates the application of another algorithm used in digital signal processing: the Walsh-Hadamard transform (WHT). This method provides a 48 % time saving because it requires only elementary algebraic operations. The study presents the results obtained processing 30 blood-pool cardiac acquisitions in various diseases. No significant difference was found in the pairs of maps and in the parameters chosen for comparison of the data.

J Nucl Med 25: 608-612, 1984

The clinical use of amplitude and phase maps to evaluate gated blood-pool studies currently appears to be a widespread method of displaying abnormalities of cardiac contraction (1-4). Though some inaccuracies have been pointed out (5), first-harmonic Fourier analysis is currently used as proposed by Adam et al. (6) in 1979.

It is well known that this technique uses a sinusoidal curve to fit the behavior of single-pixel activity in a sequence of frames representing an average cardiac cycle. In this way it is possible to draw local values of amplitude and phase in order to get parametric images.

The calculation of such parameters with the computers normally used in nuclear medicine is time-consuming. We have investigated the possibility of obtaining the results of temporal Fourier analysis by applying a different algorithm based on the Walsh-Hadamard transform (WHT), which is well known in digital signal processing and has already been proposed for nuclear medicine data compression (12,13).

METHODS

The WHT is the best known of the nonsinusoidal orthogonal transforms (7). It has gained widespread use in digital signal processing, since its application is easy and it shortens processing time.

The WHT shares the following characteristics with the discrete Fourier transform (DFT) (8,9):

1. It has to do with periodic finite series and provides a spectrum whose period contains the same sample number as the temporal sequence.

2. It uses fast and efficient methods to compute the algorithm, with few operations.

3. It can be extended to multidimensional signals.

In addition, the WHT has the following advantages: (a) its nature is real, and (b) only additions and subtractions are required to compute the coefficients.

The Walsh functions. The Walsh functions, designated $wal(i, t)$, are rectangular waves, periodical or not, involving only two values (± 1) (Fig. 1).

The set of Walsh functions, like the Fourier set, forms an orthonormal, closed system (7,10). Therefore every function $f(t)$ that is absolutely integrable in the fundamental interval $T[\int_0^T |f(t)| dt < \infty]$ can be expanded in a Fourier or Walsh convergent series.

The Walsh functions, $wal(i, t)$, are alternately odd and even (named sal and cal) with the respect to the central point:

$$wal(i, t) = cal(s, t) \text{ when } i \text{ is even}$$

$$wal(i, t) = sal(s, t) \text{ when } i \text{ is odd.}$$

In $wal(i, t)$ the functions from the $sal(3, t)$ often have cycles of different length (Fig. 1). Hence the frequency concept, which is significant in sinusoidal Fourier waves, is not applicable in this case and can be replaced by the concept of Sequence s .

The Hadamard functions [$had(l, t)$] are the $wal(i, t)$ rearranged in different order.

The Walsh-ordered Walsh-Hadamard transform (WHT)_w. This form is applicable when the sequences associated with the transform coefficients are needed in a natural increasing order.

The (WHT)_w of a series of $N = 2^n$ samples,

Received July 14, 1983; revision accepted Nov. 9, 1983.

For reprints contact: Dr. Piero Morello, Cattedra di Medicina Nucleare, C/so Polonia 14, 10100 Torino, Italy.

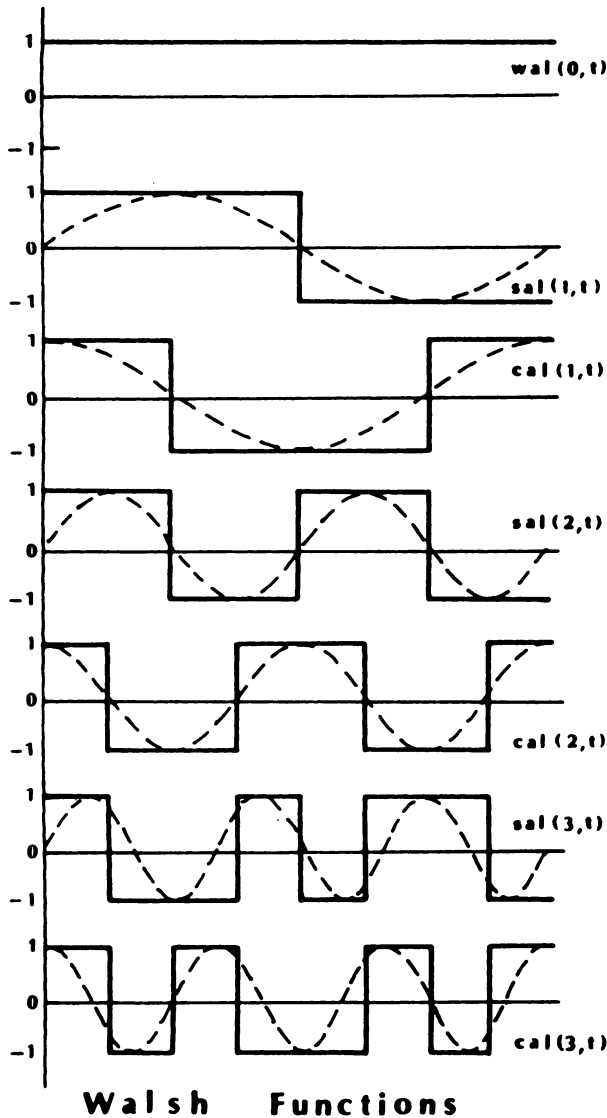


FIG. 1. Walsh functions are shown, with corresponding Fourier sinusoids (dashed lines). In lowest pair, correspondence between waves deteriorates.

$$\bar{X}(n) = [X(0)X(1) \dots X(N - 1)],$$

is given by:

$$\bar{W}(n) = \frac{1}{N} M_w(n) \bar{X}(n)$$

where $M_w(n)$ is an $(N \times N)$ orthogonal, symmetric Walsh-ordered matrix, obtained by sampling the first N $wal(i, t)$ N times.

The inverse transform $(I\bar{W}T)_w$ is defined as:

$$\bar{X}(n) = M_w(n) \bar{W}(n).$$

For example, for $N = 8$, $M_w(3)$ results in:

$$M_w(3) = \begin{bmatrix} 1 & 1 & 1 & 1 & 1 & 1 & 1 & 1 \\ 1 & 1 & 1 & 1 & -1 & -1 & -1 & -1 \\ 1 & 1 & -1 & -1 & -1 & -1 & 1 & 1 \\ 1 & 1 & -1 & -1 & 1 & 1 & -1 & -1 \\ 1 & -1 & -1 & 1 & 1 & -1 & -1 & 1 \\ 1 & -1 & -1 & 1 & -1 & 1 & 1 & -1 \\ 1 & -1 & 1 & -1 & -1 & 1 & -1 & 1 \\ 1 & -1 & 1 & -1 & 1 & -1 & 1 & -1 \end{bmatrix}$$

The fast Walsh-Hadamard transform $(FWHT)_w$. To compute the N coefficients of $(WHT)_w$, N^2 additions and subtractions are required. As in the Fourier transform, there is an algorithm, called the fast Walsh-Hadamard transform $(FWHT)_w$, that yield the coefficients $W(n)$ in $N \log_2 N$ additions and subtractions (i.e., for $N = 8$, the number of operations falls from 64 to 24). It permits computation of the $(WHT)_w$ efficiently. A current version, which uses a Cooley type of flow graph, was introduced by Manz (8,9,14).

DFT and $(WHT)_w$ amplitude and phase values. The discrete Fourier transform of a function f at the frequency k with N samples is given by:

$$F(k) = \sum_{n=0}^{N-1} f(n) \exp(-j2\pi kn/N) = \sum_{n=0}^{N-1} f(n) \cos(2\pi kn/N) - j \sum_{n=0}^{N-1} f(n) \sin(2\pi kn/N).$$

The real portion $R(k)$ and the imaginary portion $I(k)$ are given by:

$$R(k) = \sum_{n=0}^{N-1} f(n) \cos(2\pi kn/N),$$

$$I(k) = \sum_{n=0}^{N-1} f(n) \sin(2\pi kn/N). \quad (1)$$

Finally, the amplitude $A(k)$ and the phase $P(k)$ are defined as:

$$A(k) = \frac{1}{N} [R(k)^2 + I(k)^2]^{1/2},$$

$$P(k) = \text{arctg}[I(k)/R(k)]. \quad (2)$$

The same subdivision into real and imaginary parts does not apply to $(WHT)_w$ coefficients, all of which are real. They are, however, alternatively distinguishable in even-valued terms W_e (as the cosine function) and odd-valued terms W_o (as the sine function).

Hence the N -vector $\bar{W}(n)$ is separable, with increasing s , into two groups of terms given by:

$$W_o(2s - 1) = \frac{1}{N} \sum_{i=0}^N \text{sal}_d(s, i) X(i)$$

$$W_e(2s) = \frac{1}{N} \sum_{i=0}^N \text{cal}_d(s, i) X(i), \quad (3)$$

where $\text{cal}_d(s, i)$ and $\text{sal}_d(s, i)$ are the discrete even and odd Walsh functions at the sequence s .

The amplitude $A(s)$ and phase $P(s)$, at the sequence s are given by:

$$A(s) = [W_o^2(2s - 1) + W_e^2(2s)]^{1/2}$$

$$P(s) = \text{arctan}[W_o(2S - 1)/W_e(2s)]. \quad (4)$$

Comparison between DFT and $(WHT)_w$. The two sets of base functions have the same properties, but their shapes are different. Like the results reported in the literature (13), the two transforms in first harmonic differ in a constant value (the sine and cosine always have, during the period, two zero-valued points, whereas the Walsh functions always have nonzero values).

To assess this difference we fitted a cosinusoidal wave as $A \cos(\omega t + \varphi)$ to the DFT and $(WHT)_w$ first-harmonic component. The pairs of amplitude values $(A_{DFT}, A_{(WHT)_w})$ and phase values $(\varphi_{DFT}, \varphi_{(WHT)_w})$ were calculated from the formulas in the previous paragraph for $K = 1$ and $s = 1$.

This revealed (a) an amplitude increase of 28% for the Walsh Transform, and (b) a phase shift of 11° .

We proceeded to apply the same procedure to experimental volume curves from our patient population, and obtained the same results (Fig. 2).

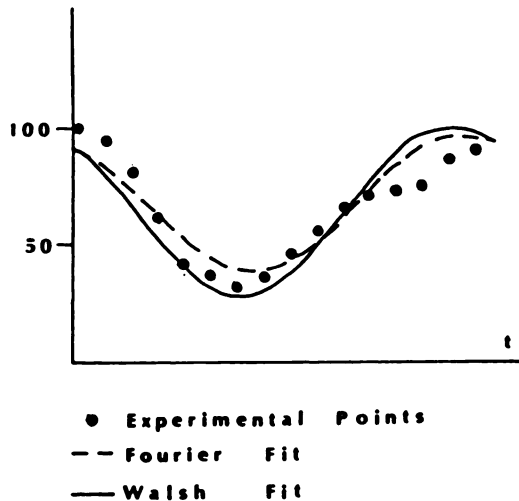


FIG. 2. Comparison of first-harmonic fits to left-ventricular volume curve. DFT and $(WHT)_w$ curves were drawn using formula: $f(t) = A \cos(\omega t + \varphi)$, with $A = A_{DFT}$, $A_{(WHT)_w}$ and $\varphi = \varphi_{DFT}$, $\varphi_{(WHT)_w}$. 16 experimental points, with maxima normalized to 100, are derived from study of our patient population.

Software development. For input, the program that applies the first-harmonic Fourier analysis needs a 16- or 24-frame study (64×64) and provides an output of two 64×64 images (amplitude and phase maps). The algorithm used is the trigonometric form of DFT, where Eqs. (1) and (2) have been applied with $K = 1$ and $N = 16, 24$.

Our system has no floating-point processor, but the involved approximation was considered wholly satisfactory. We reduced the execution time further by using preformed trigonometric tables.

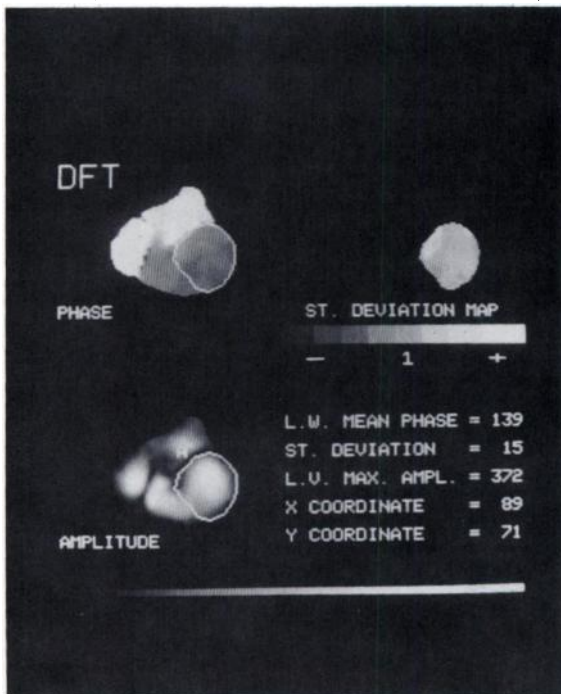


FIG. 3. Visual results of DFT fit, including values of parameters used for comparison, derived from a patient with no evident wall-motion abnormalities and good resting ejection fraction (51%).

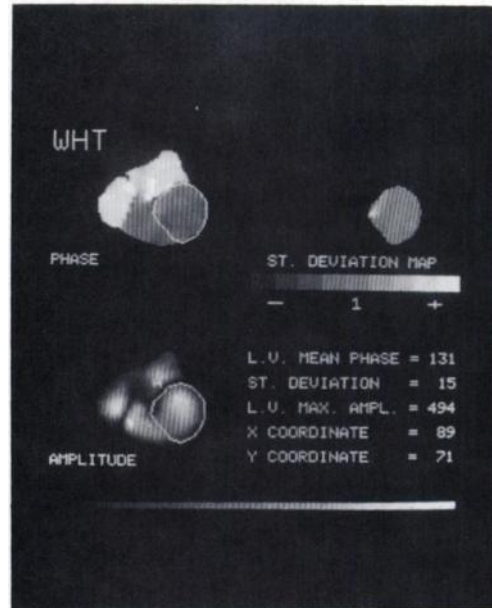


FIG. 4. Data of Fig. 3 processed with WHT fit.

The program was carried out according to rules of "structured programming" (15), whose block feature allowed easy insertion of the WHT technique into the preexisting program. For this algorithm we used Eqs. (3) and (4) with $s = 1$ and $N = 16, 24$. The preformed trigonometric tables were not utilized, since this technique needs only additions and subtractions among the N samples. Moreover, in neither case did we use methods for speeding up the transforms (FFT, FWHT). In fact, in calculating a single harmonic (the first in our case), there is no advantage in using FFT instead of DFT (or FWHT instead of WHT) because the number of operations is the same.

RESULTS AND DISCUSSION

We have compared the results of the two algorithms (DFT and WHT) in 30 blood-pool gated ventriculograms from 18 patients (18 studies at rest and 12 during stress, one of which followed nitroglycerin administration). Data acquisition was performed using a slant-hole collimator (30°), in the left anterior oblique projection, for a period of 10–12 min at rest and for 3–5 min during stress (with a bicycle at the submaximal step). The counts were collected in frame mode (16 frames in 64×64 matrix), synchronized by the R wave according to our normal gating procedure.

Clinically the patients fell into four groups: (a) 12 with confirmed or suspected coronary disease (20 studies: 12 at rest, eight during stress); (b) two with aortic insufficiency (four studies: two at rest, two during stress); (c) two had received permanent pacemakers (three studies: two at rest, one during stress); (d) two with cardiomyopathy (three studies: two at rest, one during stress).

The 16-frame sequence, representing an average cardiac cycle, always underwent two steps of spatial smoothing with a 9-point filter (3×3 matrix, weights 4, 2, 1). Subsequently the left-ventricular ejection fraction was calculated; in our population it varied from 13 to 80.7%. This large dispersion was chosen intentionally to test DFT and WHT in the different circumstances of clinical practice. From every case, using the first-harmonic coefficients derived by the two algorithms, we obtained a pair of amplitude and phase maps, in 64×64 matrix, as well as the phase distribution histograms. By interpolation, the images were displayed in 128×128 format for easier evaluation.

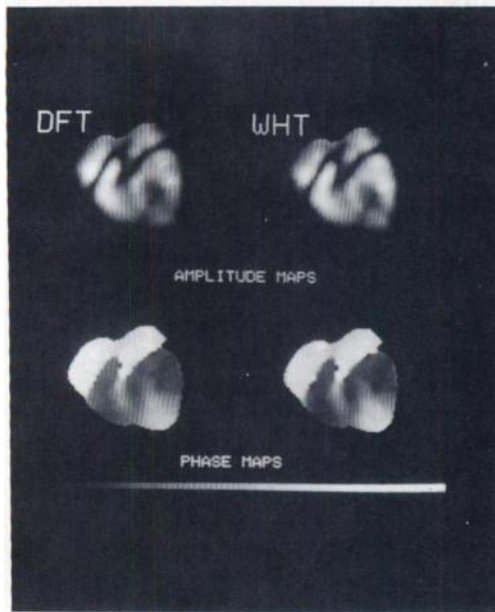


FIG. 5. DFT and WHT amplitude and phase images, from patient with severe reduction of left-ventricular ejection fraction (20%). Apical dyskinetic region is evident (confirmed aneurysm).

For further analysis, we derived the mean and standard deviation of the phases inside a left-ventricular ROI, previously defined in order to estimate the ejection fraction. The deviation of each pixel from the mean was weighted and stored as a discrete s.d. value ($\pm 1, \pm 2, \pm 3$, etc.). Thus, we were able to construct a left-ventricular map where different colors or gray levels coded all pixels with the same s.d. value (points lying between -1 to $+1$ s.d. were displayed as a single level).

Computing time. By computing time, we mean the time necessary to create a pair of parametric images (phase and amplitude)

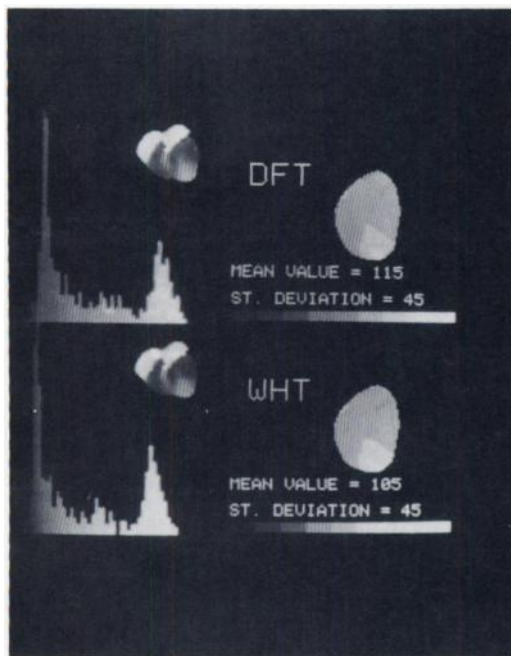


FIG. 6. Phase-distribution histograms and standard deviation maps derived from patient of Fig. 5.

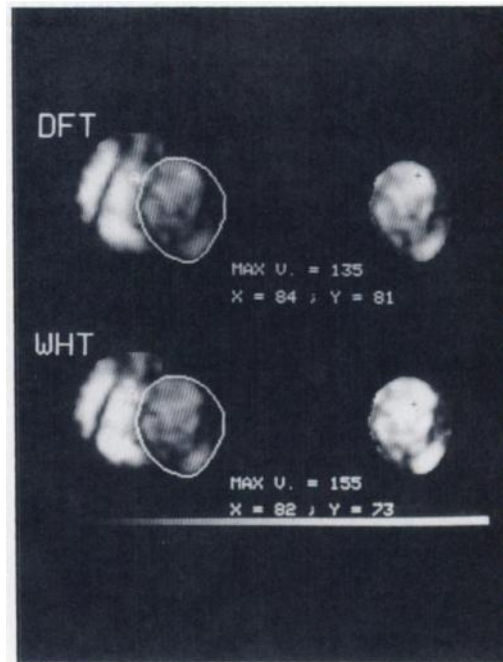


FIG. 7. Amplitude maps from patient with enlarged, hypokinetic left ventricle. Disagreement in position of pixel with maximum amplitude does not affect clinical evaluation.

by processing the 16 frames representing a mean cardiac cycle, in 64×64 format. In order to get comparable results, our tests were always carried out using the initial sectors of a 5-Mbyte magnetic cartridge (our computer is equipped with a 5- + 5-Mbyte disk unit).

For the theoretical reasons previously expressed, the computing times for DFT and WHT were significantly different (see Table 1), with the WHT procedure showing a mean advantage equivalent to 39.6%. The related times included I/O operations, exactly the same for both the programs, which consumed 16 sec. If we subtract this constant value, not strictly pertaining to the computing procedure, we find that the real time-saving of the WHT algorithm reaches 48% with our operating conditions.

Clinical evaluation. The parametric images showed the following results: 13 cases with no evident abnormalities of amplitude and phase (43.4%), 11 with various degrees of hypokinesia (36.7%), six with dyskinetic regions (20%), two of which were recognized as aneurysm by contrast ventriculography.

Looking over the parametric images obtained with the two techniques, we find complete agreement, as clearly appears in Figs. 3-6. Figures 7 and 8 are from the patient study with the worst comparison between DFT and WHT. They show an enlarged left ventricle, with a wide dyskinetic region involving the anterolateral wall; there was a severe depression of the ejection fraction to 13%. In this study there are small differences, not very significant, and only in the amplitude map (Fig. 7).

In some cases we tested the agreement of the phase values by cross-subtraction (DFT minus WHT image or vice versa), after we had balanced the phase shift of the WHT algorithm. The resulting maps showed nonzero values only outside the cardiac area.

Quantitative analysis. To quantify the results, we used the same ROI, previously defined over the left ventricle, to calculate the following parameters from the DFT and WHT images:

- (a) the mean value of the phase,
- (b) its standard deviation,
- (c) the maximum value in the amplitude image,

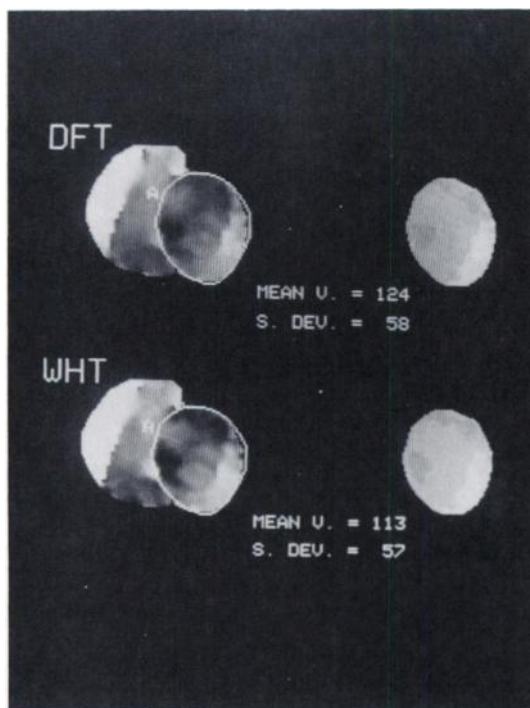


FIG. 8. Phase maps from patient of Fig. 7. Large dyskinetic area is well defined by both techniques.

(d) the coordinates of the pixel in which each maximum appeared.

The comparative data for the 30 studies are listed in Table 1.

We must emphasize the very close correlation found in every comparison of the considered parameters. The differences between the mean phase values and the maxima of the amplitudes in the maps were close to those we theoretically expected (10° and 28% in counts per pixel). This fact does not affect the display of amplitudes at all, due to the normalization of the maximum values in each image; the phase shift can at worst result in two display levels, since the 360° possible values were sampled by the software program every 6° and were coded in 60 colors or gray levels (the scale is shown in the pictures).

Concerning the coordinates of the pixel with the maximum amplitude value, we observed the correct coincidence in 21 studies (70%). The other nine—all belonging to patients with poor ejection fraction—showed very small shifts. Figures 7 and 8 display the study with the greatest disagreement, but we may mention that for the point with the maximum DFT amplitude there was a corresponding WHT value equal to 97% of the corresponding maximum. This difference is not visually appreciable.

CONCLUSIONS

Our results confirm that WHT is a computing technique that gives clinical information closely correlated with the DFT analysis of first-harmonic fitting. We think, therefore, that it may provide an alternative method of processing gated data.

The special aspects of WHT are the saving of time (48% compared with DFT for our algorithms) and the ease of calculation. These properties suggest further applications of WHT both in multiharmonic analysis and in the spatial and temporal filtering of the digital images.

FOOTNOTE

* Medusa 12/B-SEPA, TURIN.

ACKNOWLEDGMENT

The authors thank N. Miletto for his assistance in software development.

REFERENCES

1. BYROM E, PAVEL DG, SWYRIN S, et al: Phase images of gated cardiac studies: A standard evaluation procedure. In *Functional Mapping of Organ Systems and Other Computer Topics*. Esser PD, ed. New York, The Society of Nuclear Medicine, 1981, pp 129-138
2. BACHARACH SL, GREEN MV, DE GRAAF CN, et al: Fourier phase distribution maps in the left ventricle: Toward an understanding of what they mean. In *Functional Mapping of Organ Systems and Other Computer Topics*. Esser PD, ed. New York, The Society of Nuclear Medicine, 1981, pp 139-148
3. RATIB O, HENZE E, SCHÖN H, et al: Phase analysis of radionuclide ventriculograms for the detection of coronary artery disease. *Am Heart J* 104:1-12, 1982
4. SWYRIN S, PAVEL DG, BYROM E, et al: Sequential regional phase mapping of radionuclide gated biventriculograms in patients with sustained ventricular tachycardia: Close correlation with electrophysiologic characteristics. *Am Heart J* 103:319-332, 1982
5. WENDT RE III, MURPHY PM, CLARK JW JR, et al: Interpretation of multigated fourier functional images. *J Nucl Med* 23:715-724, 1982
6. ADAM WE, TARKOWSKA A, BITTER F, et al: Equilibrium(gated) radionuclide ventriculography. *Cardiovasc Radiol* 2:161-173, 1979
7. SZEGÖ G. *Orthogonal Polynomials*. Providence, Rhode Island, American Mathematical Society, 1939. (Fourth edition 1975), pp 23-57
8. OPPENHEIM AV, SCHAFER RW: *Digital Signal Processing*. Englewood Cliffs, Prentice Hall, 1979, pp 356-383
9. LIFERMANN J: *Les méthodes rapides de transformation du signal: Fourier, Walsh, Hadamard*, Haar. Masson, Paris, 1979, pp 162-175
10. AHMED N, RAO KR: *Orthogonal transforms for digital signal processing*. New York, Springer-Verlag, 1975, pp 99-131
11. LINKS JM, DOUGLASS KM, WAGNER MN JR: Patterns of ventricular emptying by Fourier analysis of gated blood-pool studies. *J Nucl Med* 21:978-982, 1980
12. DECONINCK F, BOSSUYT A, LEPOUDRE R, et al: The use of the temporal Hadamard transform for efficient data compression during image acquisition and processing. *J Nucl Med* 22:P 13-14, 1981 (abst.)
13. DECONINCK F, BOSSUYT A, LEPOUDRE R: New approaches for the analysis and visualisation of time patterns of dynamic scintigraphic imaging. In *Nuclear Medicine and Biology Proceedings of the Third World Congress of Nuclear Medicine and Biology*. Vol. 1, Raynaud C, Ed. Pergamon, 1982, pp 39-41
14. MANZ JW: A sequency-ordered Fast Walsh Transform. *IEEE Trans Audio Electroacoust* AU-20 204-205, 1972
15. MCGOWAN CL, KELLY JR: *Top-Down Structured Programming Techniques*. Petrocelli Books, 1975